Article

Comparative Study of Green's Function Matrix Elements and Charge Transfers Obtained from Different Partitioning Schemes of Molecular Charge in Hydrogen-Bonded Complexes

Antenor J. Parnaíba-da Silva, João Bosco P. da Silva, A. Arnóbio S. da Gama and Mozart N. Ramos[*]

Departamento de Química Fundamental - Universidade Federal de Pernambuco, 50740-540 Recife-PE, Brazil

Cálculos de orbitais moleculares *ab initio* RHF e MP2 usando os conjuntos de base 4-31G**, 6-311G** e cc-pVTZ têm revelado que os valores de $G_{D,A}$ mostram uma boa correlação com transferências de cargas atômicas intermoleculares obtidas a partir de diferentes esquemas de partição para os complexos de hidrogênio CNH…CNH, NCH…CNH, CNH…NCH e NCH…NCH. Isto é especialmente evidente quando a distância da ligação de hidrogênio é progressivamente aumentada até 4,5 Å. Entretanto, valores de $G_{D,A}$ mostram uma melhor correlação linear com valores de ΔQ usando as cargas Mülliken corrigidas, que são obtidas do modelo carga-fluxo de carga-recobrimento (CCFO) para intensidades no infravermelho. Neste caso, ambos $G_{D,A}$ e ΔQ formam duas curvas exponenciais praticamente superpostas. Por outro lado, valores de $G_{D,A}$ mostram uma menor concordância com valores de ΔQ obtidos das cargas atômicas derivadas dos orbitais de ligação naturais. Isso é claramente verificado quando é considerada a taxa de decaimento exponencial de primeira ordem de $G_{D,A}$ *versus* ΔQ obtida de diferentes esquemas de partição de carga.

RHF and MP2 *ab initio* molecular orbital calculations using the 4-31G**, 6-311G** and cc-pVTZ basis sets have revealed that the Green's function matrix element ($G_{D,A}$) values show a good correlation with the amount of intermolecular transferred charges obtained from different charge partitioning schemes for the CNH…CNH, NCH…CNH, CNH…NCH and NCH…NCH hydrogen bonded complexes. This is evident specially when the hydrogen bond distance is progressively increased from the equilibrium position until 4.5 Å. However, $G_{D,A}$ values show a better linear correlation with ΔQ values using corrected Mülliken charges, which are obtained from the charge-charge flux-overlap (CCFO) model for infrared intensities. In this case, both $G_{D,A}$ and ΔQcorr form two practically superposed exponential curves. On the other hand, $G_{D,A}$ values show a smaller agreement with ΔQ values obtained from atomic charges derived from natural bonding orbitals. This is clearly verified when considering the first order exponential decay rate of $G_{D,A}$ versus ΔQ obtained from different charge partitioning schemes.

Keywords: hydrogen bond, *ab initio* calculations, charge transfer, Green´s function, atomic charge partitioning

Introduction

When a hydrogen-bonded complex is formed, an intermolecular charge transfer occurs, and its magnitude is sometimes directly associated with the hydrogen bond strength.[1] Currently, this charge transfer is obtained from atomic charges derived from *ab initio* molecular orbital calculations with different basis sets. These charges can be computed from different partitioning schemes of molecular charge. This procedure may suggest a qualitative idea of the magnitude of

intramolecular and intermolecular interactions and of chemical reactivity at various sites within the molecule. Often quantitative predictions can be made on the same basis. In particular, atomic charges derived from the charge-charge flux-overlap (CCFO) model[2] for infrared intensities have been useful to predict such interactions in hydrogen bonded complexes.[3,4] Indeed, the so-called corrected Mulliken atomic charges[5] are calculated by adding a specific element of the overlap tensor of the CCFO model to the standard Mulliken charges. More recently, we have shown[6] that charge transfers obtained from corrected Mulliken charges (ΔQcorr) are linearly correlated with a Green's function matrix elements

* e-mail: mramos@ufpe.br

$(G_{D,A})$[7] in hydrogen-bonded complexes of the $C_nNH...C_nNH$ and $C_nNH...NC_nH$ (n = 1 and 3) type. The Green's function formalism was introduced as a tool for the calculation of bridge mediated donor-acceptor interactions $V_{da} = V_{dD} G_{DA} V_{Aa}$[7] that appears in the Fermi's Golden Rule expression of a diabatic electron transfer rate, $k = \frac{2\pi}{\hbar}|V_{da}|^2 (FC)$[8] and molecular wire conductance.[9] Then, a correlation is observed among the charge transfer probability and the magnitude of the charge transferred upon the formation of the H-bond.

There we have verified that the larger is the intermolecular charge transfer for a given complex, the larger its $G_{D,A}$ value appears to be. We have also noted that $G_{D,A}$ and $\Delta Qcorr$ are associated with the binding energies of these complexes. Furthermore, both $G_{D,A}$ and $\Delta Qcorr$ show the same behavior when the hydrogen bonding distance is progressively increased from the equilibrium position until 4.5 Å, forming two practically superposed exponential curves.

It is also interesting to point out that hydrogen bonding is believed to play an important hole in electron transfer. An electron tunneling pathway model, described as a sequence of covalent, hydrogen bonding and through space interactions, was developed and applied for the reproduction and prediction of electron transfer rates in modified metalloproteins.[10] Some molecular model systems with hydrogen bonding on the pathway from electron donor to electron acceptor have been designed for experimental studies.[11] The behavior of $G_{D,A}$ through this hydrogen bonding bridge was compared with covalent saturated and unsaturated bridges and indeed it shows a faster decay with the separation distance.[12]

In this paper we intend to compare $G_{D,A}$ values with intermolecular charge transfers obtained from different partitioning schemes of molecular charge. Besides the corrected Mulliken charges[5], we also consider the standard Mulliken charges[13], atomic charges derived from electrostatic potentials[14] and those obtained from natural bonding orbitals.[15] This comparative study will be performed on the CNH...CNH, NCH...CNH, CNH...NCH and NCH...NCH complexes employing RHF[16] and MP2[17] *ab initio* molecular orbital calculations with the 4-31G**[18], 6-311G**[19] and cc-pVTZ[20] basis sets.

Calculations

The procedures to obtain Green's function matrix elements and the corrected Mulliken charges are given in References 6 and 5, respectively. The *ab initio* calculations

were performed with the GAUSSIAN 94 program.[21] In this procedure, the molecular geometry of the isolated molecules and their hydrogen-bonded complexes at the equilibrium distance were fully optimized and no imaginary frequency was observed. The MP2 calculations were performed using the electron frozen core approximation. It is also important to call attention that the $G_{D,A}$ values were calculated using natural bonding orbitals while s and p atomic orbitals or hybrids were used as intermediate steps on the construction of these natural orbitals. These later have been shown to be more adequate in analyzing electron transfer interaction propagation.[22]

The MP2/4-31G** optimized geometries of CNH... CNH, NCH...CNH, CNH...NCH and NCH...NCH complexes and their monomers are given in Figure 1. The internal default criteria of Gaussian 94 were used in all calculations.
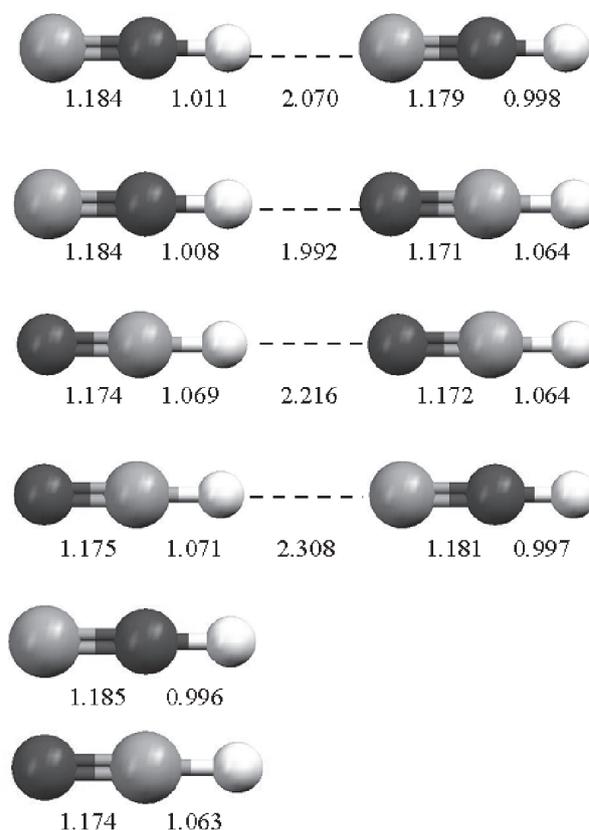
Figure 1. MP2/4-31G** optimized geometries of CNH...CNH, CNH...NCH, NCH...NCH, and NCH...CNH complexes and the CNH and NCH monomers. Bond distances in Angstrom.

Results and Discussion

Table 1 shows $G_{D,A}$ and ΔQ values using the MP2 and RHF levels of calculation with the 4-31G**, 6-311G** and cc-pVTZ basis sets for the CNH...CNH, NCH...CNH, CNH...NCH and NCH...NCH complexes. Here ΔQ is

the amount of transferred atomic charge from a molecule to another when the hydrogen bond is formed. This quantity is obtained from four different partitioning schemes of molecular charge: (*i*) $\Delta Q corr$ is obtained from the corrected Mulliken charges using the charge- charge flux-overlap (CCFO) model for infrared intensities; (*ii*) ΔQ_M is calculated from the traditional Mulliken charges; (*iii*) ΔQ_{CHELPG} is obtained from atomic charges derived from electrostatic potentials and, finally, (*iv*) ΔQ_{NBO} is obtained from atomic charges using natural bonding orbitals. Initially, we can note from Table 1 that the $G_{D,A}$ values show a good correlation with the ΔQ values for these four different partitioning schemes of molecular charge. In general, we can verify that the larger is the Green's function matrix elements ($G_{D,A}$) for a given complex, the larger its corresponding charge transfer appears to be. This can be visualized in Figure 2 considering $G_{D,A}$ and ΔQ_{CHELPG} values for the four
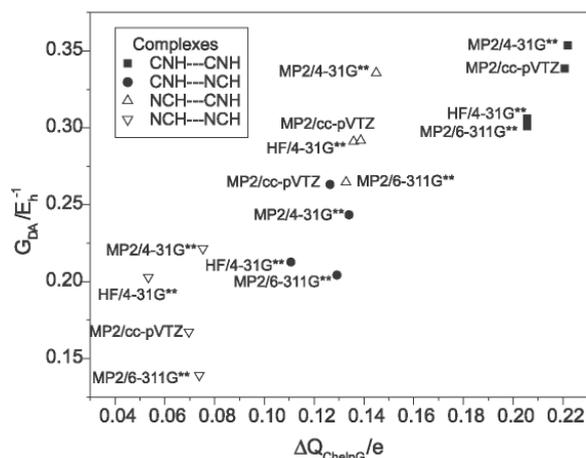
Figure 2. Graph of $G_{D,A}$ versus ΔQ_{CHELPG} for the CNH...CNH, NCH...CNH, CNH...NCH and NCH...NCH complexes using given in Table 1.

hydrogen-bonded complexes here employed using the RHF/4-31G**, MP2/4-31G**, MP2/6-311G** and MP2/cc-pVTZ calculations.

For example, $G_{D,A}$ values using the MP2/4-31G** calculation level for the CNH...CNH, NCH...CNH, CNH...NCH and NCH...NCH complexes are 0.354 E_h^{-1}, 0.336 E_h^{-1}, 0.244 E_h^{-1} and 0.222 E_h^{-1}, respectively, whereas their corresponding values for ΔQ_{CHELPG} are 0.222 e, 0.145 e, 0.134 e and 0.075 e, respectively. We have also investigated a possible correlation between $\ln G_{D,A}$ values and $r_{H...X}$ hydrogen bond lengths involving the hydrogen-bonded complexes here studied. However, our results show that these parameters are not correlated. While $\ln G_{D,A}$ values follow the order: CNH...CNH > NCH...CNH > CNH...NCH > NCH...NCH, as can be seen in Table 1, the hydrogen bond lengths, in turn, follow the order: NCH...CNH > NCH...NCH > CNH...CNH > CNH...NCH. This later can be seen in considering the $r_{H...X}$ values obtained from the MP2/4-31G** calculations shown in Figure 1.

$G_{D,A}$ values always follow for a given calculation the order: CNH...CNH > NCH...CNH > CNH...NCH > NCH...NCH. However, some inversions are found for the values of the intermolecular charge transfers involving the NCH...CNH and CNH...NCH complexes. For example, $G_{D,A}$ values for NCH...CNH and CNH...NCH are 0.265 E_h^{-1} and 0.204 E_h^{-1}, respectively, using the MP2/4-31G** calculation whereas their corresponding $\Delta Q corr$ values are 0.048 e and 0.065 e, respectively. Although the trend is always consistent for the CNH...CNH and NCH...NCH complexes, some inversions occur for the NCH...CNH and CNH...NCH complexes. It is also important to point out that RHF/4-31G** calculations show $G_{D,A}$ and ΔQ values smaller than its MP2/4-31G** corresponding values. For example, the $G_{D,A}$ values using

Table 1. $G_{D,A}$ and ΔQ values for the CNH...CNH, NCH...CNH, CNH...NCH and NCH...NCH complexes using the MP2 and RHF calculations levels with the 4-31G**, 6-311G** and cc-pVTZ basis sets

Complexes	Calculation	$G_{D,A}(E_h^{-1})$	ΔQ_{Corr} (e)	ΔQ_M(e)	ΔQ_{CHELPG}(e)	ΔQ_{NBO}(e)
CNH...CNH	RHF/4-31G**	0.306	0.072	0.060	0.205	0.031
	MP2/4-31G**	0.354	0.095	0.074	0.222	0.052
	MP2/6-311G**	0.301	0.084	0.052	0.206	0.042
	MP2/cc-pVTZ	0.339	0.092	0.061	0.221	0.049
NCH...CNH	RHF/4-31G**	0.291	0.053	0.046	0.136	0.018
	MP2/4-31G**	0.336	0.066	0.052	0.145	0.029
	MP2/6-311G**	0.265	0.048	0.036	0.133	0.017
	MP2/cc-pVTZ	0.292	0.055	0.040	0.139	0.022
CNH...NCH	RHF/4-31G**	0.213	0.048	0.030	0.111	0.017
	MP2/4-31G**	0.244	0.063	0.048	0.134	0.032
	MP2/6-311G**	0.204	0.065	0.046	0.134	0.026
	MP2/cc-pVTZ	0.263	0.075	0.053	0.129	0.029
NCH...NCH	RHF/4-31G**	0.203	0.037	0.023	0.053	0.010
	MP2/4-31G**	0.222	0.044	0.035	0.075	0.015
	MP2/6-311G**	0.139	0.041	0.035	0.074	0.012
	MP2/cc-pVTZ	0.167	0.047	0.032	0.070	0.013

the RHF/4-31G** level of calculation are 0.306 E_h^{-1}, 0.291 E_h^{-1}, 0.213 E_h^{-1} and 0.203 E_h^{-1} for the CNH…CNH, NCH…CNH, CNH…NCH and NCH…NCH complexes, respectively, whereas their MP2/4-31G** corresponding values are 0.354 E_h^{-1}, 0.336 E_h^{-1}, 0.244 E_h^{-1} and 0.222 E_h^{-1}, respectively.

The larger values for both $G_{D,A}$ and ΔQ are verified for the CNH…CNH complex, whereas their smaller values are verified in NCH…NCH. This can be understood in considering the greater acid character of CNH with respect
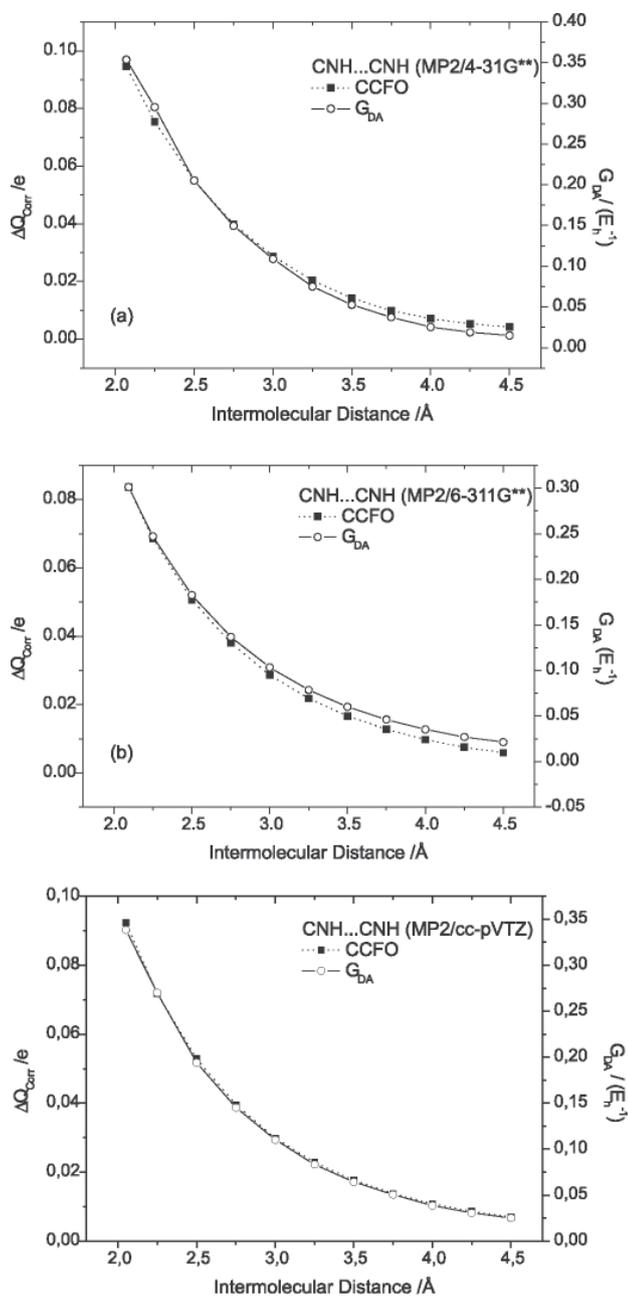
Figure 3. Graphs of $G_{D,A}$ and ΔQcorr as function of the hydrogen bonding distance in the CNH…CNH complex using the MP2 calculation level with the (a) 4-31G**, (b) 6-311G** and (c) cc-pVTZ basis sets.

to NCH. In this sense, it is also interesting to take into account their HOMO and LUMO energies. The values of ε_{HOMO} and ε_{LUMO}, for CNH are –13.363 eV and 3.608 eV, respectively, using the MP2/cc-pVTZ calculation level whereas its corresponding values for NCH are –13.374 eV and 3.848 eV, respectively. The energy gap for CNH is 16.970 eV, whereas for NCH is 17.223 eV. Therefore, the charge transfer in CNH…CNH is larger than in NCH…CNH. Furthermore, this transfer is larger in CNH…NCH than in NCH…NCH.

We have already verified[6] that both $G_{D,A}$ and ΔQcorr follow an exponential behavior when the hydrogen bonding distance is progressively increased from the equilibrium position until 4.5 Å. Indeed, their exponential curves are practically superposed for both MP2 and RHF calculation levels. Figure 3 clearly shows this behavior for the CNH…CNH complex employing the MP2 level of calculation with the 4-31G**, 6-311G** and cc-pVTZ basis sets, analogously to what was verified for the other complexes.

Furthermore, we can note in Figure 4 that this exponential behavior is also verified for the other charge partitioning schemes.

However, a still better agreement is verified when corrected Mulliken charges are used to obtain charge transfer values. This can be better understood in considering that the overlap term, which is added to standard Mulliken charge to obtain the corrected Mulliken charge of the α atom, contains electronic contributions from atomic dipoles and lone pairs.[6] As a consequence, it is expected that the corrected Mulliken charges can give a better description of the distribution of molecular atomic charge. On the other hand, it is less accentuated when NBO atomic charges are employed. This can be also visualized in Table 2 considering the first order exponential decay rate (t) of these parameters using the MP2 H-bond distance at equilibrium position with the 4-31G**, 6-311G** and cc-pVTZ basis sets. Here t is given by

$$t = -\frac{r}{\ln(\Gamma / A)} \qquad (1)$$

where r is the H-bond equilibrium distance, Γ is $G_{D,A}$ or ΔQ obtained at distance r and A is the pre-exponential factor of the fitting curve. From this Table we can observe that the exponential decay rate obtained from ΔQcorr is in better agreement with that obtained from the $G_{D,A}$ than its corresponding use of ΔQ_M, ΔQ_{CHELPG} and ΔQ_{NBO} values for the CNH…CNH, NCH…CNH, CNH…NCH and NCH…NCH complexes. The major difference has been verified for ΔQ_{NBO}.
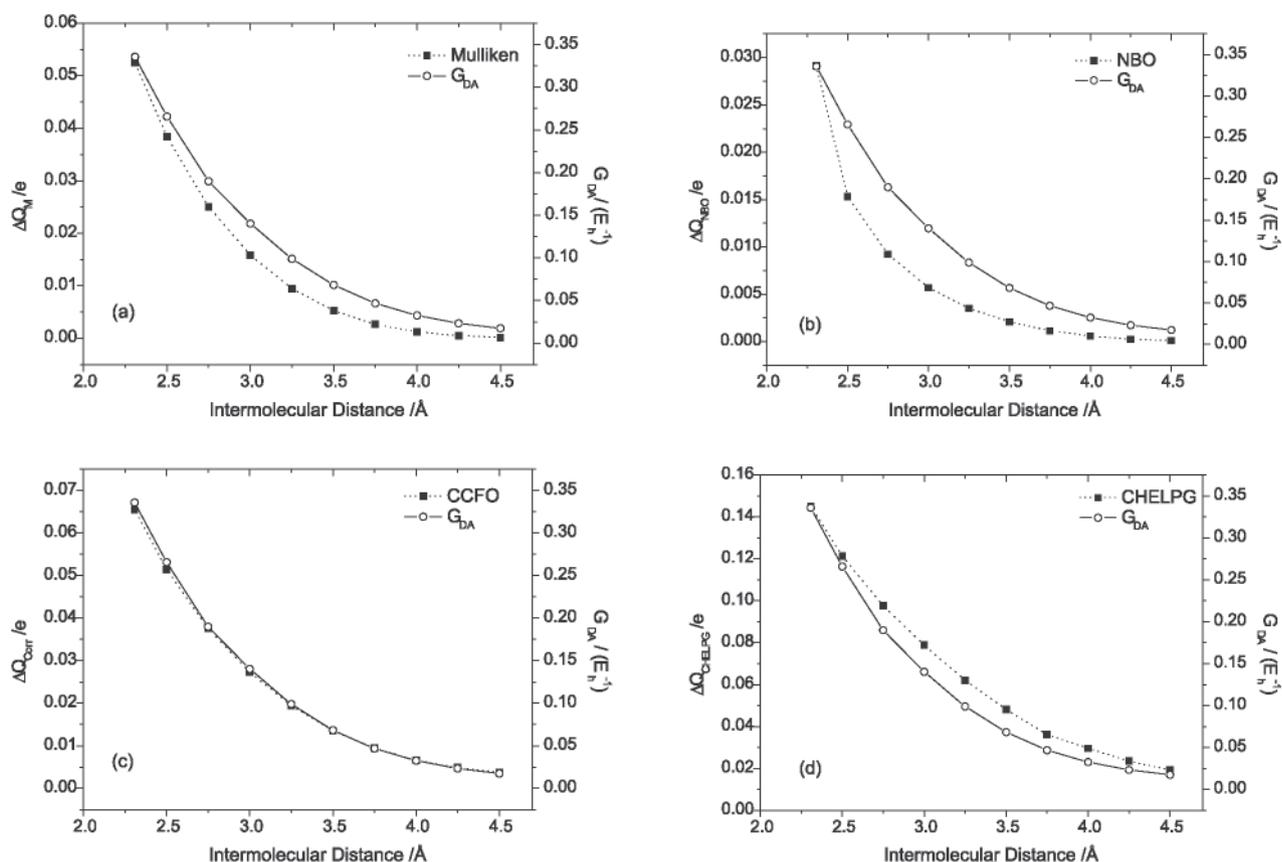
Figure 4. Graphs of $G_{D,A}$ and ΔQ as function of the hydrogen bonding distance in the NCH…NCH complex using the MP2/4-31G** level of calculation. Note that Figures 4 (a), (b), (c) and (d) use standard Mulliken charges, NBO atomic charges, corrected Mulliken charges and atomic charges obtained from electrostatic potentials, respectively.

Table 2. First order exponential decay rate (t) of $G_{D,A}$ and ΔQ with respect to calculated intermolecular distance at equilibrium position

Complexes	Calculation	t ($G_{D,A}$)	t (ΔQ_{corr})	t (ΔQ_M)	t (ΔQ_{CHELPG})	t (ΔQ_{NBO})
CNH...CNH	MP2/4-31G**	0.763	0.769	0.579	0.723	0.353
	MP2/6-311G**	0.709	0.710	0.783	0.816	0.358
	MP2/cc-pVTZ	0.700	0.698	0.717	0.795	0.361
NCH…CNH	MP2/4-31G**	0.657	0.654	0.548	0.784	0.394
	MP2/6-311G**	0.661	0.722	0.781	0.795	0.443
	MP2/cc-pVTZ	0.684	0.710	0.768	0.807	0.395
CNH…NCH	MP2/4-31G**	0.715	0.773	0.632	0.773	0.423
	MP2/6-311G**	0.650	0.686	0.776	0.787	0.359
	MP2/cc-pVTZ	0.781	0.673	0.673	0.786	0.326
NCH…NCH	MP2/4-31G**	0.736	0.665	0.614	0.806	0.454
	MP2/6-311G**	0.713	0.720	0.776	0.839	0.440
	MP2/cc-pVTZ	0.700	0.702	0.788	0.824	0.370

Conclusions

Our calculations have revealed that $G_{D,A}$ values show a good correlation with intermolecular charge transfers obtained from different partitioning schemes of molecular charge for the CNH…CNH, NCH…CNH, CNH…NCH and NCH…NCH hydrogen-bonded complexes. This is clearly verified when the hydrogen bonding distance is progressively increased from the equilibrium position until 4.5 Å. In this case, $G_{D,A}$ values show a very similar behavior with the charge transfers using corrected Mulliken charges obtained from the charge-charge flux-overlap model for infrared intensities. Indeed, $G_{D,A}$ and ΔQ_{corr} yield two exponential curves practically superposed. The first order exponential decay rate is useful to numerically express this behavior. Currently, studies are in progress in our laboratory in order to evaluate this similarity between $G_{D,A}$ and ΔQ for other hydrogen-bonded complexes.

Acknowledgments

References

1. Araújo, R. C. M. U.; Ramos, M. N.; *J. Mol. Struct. (Theochem)* **1996**, *366*, 233; Lopes, K. C.; Pereira, F. S.; Ramos, M. N.; Araújo, R. C. M. U.; *Spectrochim. Acta, Part A* **2001**, *57A*, 1339; Araújo, R. C. M. U.; Ramos, M.N.; *Spectrochim. Acta, Part A* **1995**, *51A*, 821.

2. King, W. T.; Mast, G. B.; *J. Phys. Chem.* **1976**, *80*, 2521.

3. Gussoni, M.; Castiglioni, C.; Ramos, M. N.; Rui, M.; Zerbi, G.; *J. Mol. Struct.* **1990**, *224*, 445.

4. Rui, M; Ramos, M. N.; Castiglioni, C.; Gussoni, M.; Zerbi, G.; *Mol. Cryst. Liquid Cryst.* **1990**, *187*, 275.

5. Gussoni, M.; Ramos, M. N.; Castiglioni, C.; Zerbi, G.; *Chem. Phys. Lett.* **1987**, *142*, 515; Gussoni, M.; Ramos, M. N.; Castiglioni, C.; Zerbi, G.; *Chem. Phys. Lett.* **1989**, *160*, 200.

6. Parnaíba-da-Silva, A. J.; da Silva, J. B. P.; da Gama, A. A. S.; Ramos, M. N.; *Chem. Phys. Lett.* **2002**, *362*, 159.

7. da Gama, A. A. S.; *Theor. Chim. Acta* **1985**, *68*, 159; Larsson, S.; *J. Am.Chem.Soc.* **1981**, *103,* 4034.

8. Marcus, R. A.; Sutin, N.; *Biochim. Biophys. Acta* **1985**, *811***,** 265.

9. Mujica, V.; Kemp, M.; Ratner, M. A.; *J. Chem. Phys.* **1994**, *101*, 6849.

10. Beratan, D.N.; Onuchic, J.N.; Betts, J.N.; Bowler, B.E.; Gray, H.B.; *J. Am. Chem. Soc.* **1990**, *112*, 7915.

11. de Regge, P.J.F.; Williams, S.A.; Therien, M.J.; *Science* **1995**, *269*, 1409.

12. Parnaíba-daSilva, A.J.; da Gama, A.A.S.; *Chem. Phys. Lett.* **1998**, *296*, 483.

13. Mulliken, R. S.; *J. Chem. Phys.* **1955**, *23*, 1833.

14. Cox, S. R.; Williams, D. E.; *J. Comput. Chem.* **1981**, *2*, 304; Chirlian, L. E.; Francl, M. M.; *J. Comput. Chem.* **1987**, *8*, 894.; Breneman, C. M.; Wiberg, K. B.; *J. Comput. Chem.* **1990**, *11*, 361.

15. Reed, A. E.; Weistock, R. B.; Weinhold, F. A.; *J. Chem. Phys.* **1985**, *83*, 735.

16. Atkins, P.W.; *Molecular Quantum Mechanics*, 2th ed., Oxford Press: Oxford, 1983.

17. Moller, C.; Plesset, M. S.; *Phys. Rev.* **1934**, *46*, 618.

18. Gordon, M. S.; *Chem. Phys. Lett.* **1980**, *76*, 163.

19. Raghavachari, K.; Pople, J. A.; Replogle, E. S.; Head-Gordon, M.; *J. Phys. Chem.* **1990**, *94*, 5579.

20. Kendall, R. A.; Dunning Jr., T. H.; Harrison, R. J.; *J. Chem. Phys.* **1992**, *96*, 6796.

21. Frisch, M. J.; Trucks, G. W.; Schlegel, H. B.; Gill, P. M. W.; Johnson, B. G.; Robb, M. A.; Cheeseman, J. R.; Keith, T.; Petersson, G. A.; Montgomery, J. A.; Raghavachari, K.; Al-Laham, M. A.; Zakrzewski, V. G.; Ortiz, J. V.; Foresman, J. B.; Cioslowski, J.; Stefanov, B. B.; Nanayakkara, A.; Challacombe, M.; Peng, C. Y.; Ayala, P. Y.; Chen, W.; Wong, M. W.; Andres, J. L.; Replogle, E. S.; Gomperts, R.; Martin, R. L.; Fox, D. J.; Binkley, J. S.; Defrees, D. J.; Baker, J.; Stewart, J. P.; Head-Gordon, M.; Gonzalez, C.; Pople, J. A.; *Gaussian 94, Revision E.3*, Gaussian, Inc.: Pittsburgh PA, 1995.

22. Santana, O.L.; da Gama, A.A.S.; *Int. J. Quantum Chem.* **2005**, *102*, 265.